HHS Public Access

Author manuscript

Brain Inj. Author manuscript; available in PMC 2017 March 13.

Published in final edited form as:

Brain Inj. 2016 ; 30(12): 1399–1413. doi:10.1080/02699052.2016.1219058.

Progression of tau pathology within cholinergic nucleus basalis neurons in chronic traumatic encephalopathy: A Chronic Effects of Neurotrauma Consortium Study

Elliott J. Mufson[1], **Sylvia E. Perez**[1], **Muhammad Nadeem**[1], **Laura Mahady**[1], **Nicholas M. Kanaan**[2], **Eric E. Abrahamson**[3,4], **Milos D. Ikonomovic**[3,4], **Fiona Crawford**[5], **Victor Alvarez**[6], **Thor Stein**[6], and **Ann C. McKee**[6]

[1]Dept. Neurobiology, Barrow Neurological Institute, Phoenix, AZ

[2]Dept. Translational Science and Molecular Medicine, College of Human Medicine, Michigan State University, Grand Rapids, MI

[3,4]Departments of Neurology and Psychiatry, University of Pittsburgh, Pittsburgh, PA

[4]Geriatric Research Education and Clinical Center, VA Pittsburgh Healthcare System, Pittsburgh, PA

[5]Roskamp Institute, FL

[6]VA Boston HealthCare System; Alzheimer Disease Center and CTE Program and Depts. Neurology and Pathology, Boston Univ. Sch. Med., Boston, MA

Abstract

Objective—To test the hypothesis that the nucleus basalis of Meynert (nbM), a cholinergic basal forebrain (CBF) cortical projection system, develops neurofibrillary tangles (NFTs) during the progressive pathological stages of chronic traumatic encephalopathy (CTE) in the brain of athletes.

Method—To characterize NFT pathology we used tau- antibodies marking early, intermediate, and late stages of NFT development in cholinergic basal forebrain tissue obtained at autopsy from eighteen former athletes and veterans with a history of repetitive mild traumatic brain injury (TBI).

Results—We found evidence that cholinergic nbM neurons develop intracellular tau-immunoreactive changes progressively across the pathological stages of CTE. In particular, there was an increase in pretangle (phosphorylated pS422) and oligomeric (TOC1 and TNT1) forms of tau in stage IV compared to stage II CTE cases. The nbM neurons also displayed pathologic TDP-43 inclusions and diffuse extracellular and vascular amyloid-β (Aβ) deposits in CTE. A higher percent of pS422/$p75^{NTR}$, pS422 and TNT1 labeled neurons were significantly correlated with age at symptom onset, interval between symptom onset and death and age at death.

Conclusion—The development of NFTs within the nbM neurons could contribute to the basal forebrain cortical cholinergic disconnection in CTE. Further studies are needed to determine the

Correspondence to:, Elliott J. Mufson, Ph.D., Director, Alzheimer's Disease Research Laboratory, Institutional Professor, Barrow Neurological Institute, 350 W. Thomas St., Phoenix, AZ 85013, elliott.mufson@dignityhealth.org, Phone: 602-406-8525.

Declaration of Interest:. The authors report no declarations of interest.

mechanism driving NFT formation in the nbM neurons and its relation to chronic cognitive dysfunction in CTE.

Keywords

cognition; head injury; memory; mild brain injury; traumatic brain injury

Introduction

Traumatic brain injury (TBI) is the signature wound of recent military conflicts, with 20% of U.S. service men and women sustaining at least one head injury, mainly mild TBI [1, 2]. TBI is associated with onset of long-term behavioral and cognitive problems [3] [4], but the underlying neurobiological mechanisms remain unclear. Military personnel in the battlefield and athletes in contact sports including boxing and American football [5, 6] [7] [8] [9] [10] [11] [12] are exposed to mild repetitive TBI, which can result in chronic traumatic encephalopathy (CTE). The neuropathology of CTE is characterized by intracellular accumulation of abnormally phosphorylated tau protein (p-tau), the main constituent of neurofibrillary tangles (NFT) in Alzheimer's disease (AD) and non-AD tauopathies [13]. While neuropathological investigations have demonstrated extensive cortical damage in CTE [14], the potential involvement of subcortical neurotransmitter systems is poorly understood. Among the subcortical systems displaying NFTs in AD are cholinergic neurons of the basal forebrain which provide the major acetylcholine (Ach) innervation to the cortical mantle and hippocampus and are involved in memory and cognitive functions [15] [16] [17, 18]. The cholinergic neurons within the basal forebrain are contained within several subfields extending rostrally from the septal diagonal band throughout the nucleus basalis of Meynert (nbM), caudally [18] [9]. Degenerative changes in the cortical-projecting cholinergic neurons are known to contribute to the cognitive and attentional deficits seen in AD [19] [20]. Several clinical pathological investigations report that similar pathology can develop chronically after TBI [21]. For example, the cerebral cortex of individuals who died as a consequence of head injury display reduced activity of the synthetic enzyme for Ach, choline acetyltransferase (ChAT), as well as morphological alterations and reduced ChAT immunoreactivity of the cholinergic nbM neurons [22]. TBI is also associated with acute down-regulation of the vesicular Ach transporter (VAChT, the regulator of Ach neurotransmission) and acetylcholinesterase (AChE, the Ach-degrading enzyme) [23] [24]. Moreover, several studies indicated that donepezil, an AChE inhibitor, improves cognitive function and attention after TBI [25], although this remains controversial [26] [27] [28].

The mechanism(s) driving cholinergic nbM neuronal dysfunction following CTE remain unknown. It is possible that these neurons undergo alterations of their survival protein, nerve growth factor [29, 30], which is retrogradely transported from the cortex to the nbM cholinergic neurons through a complex interaction with its two cognate receptors, the high-affinity NGF-specific cell survival tyrosine kinase (trkA) and the putative cell death associated low-affinity pan neurotrophin ($p75^{NTR}$) receptor [31] [32]. In AD, these neurons also develop intracellular lesions that appear as globose p-tau-positive NFTs [33] [13]. Tau is a microtubule-associated protein involved in normal cytoskeleton function [34] [35] and tau containing NFT pathology co-occurs within nbM neurons containing the cholinergic cell

markers ChAT and $p75^{NTR}$ early in the onset of AD [36]. Recently, a linear model for NFT evolution has been proposed, that can be observed by antibodies directed against p-tau epitopes marking early, intermediate, and late stages of NFT development during the progression of AD [37–43]. For example, tau phosphorylation at Serine 422 (pS422) was identified as an early event using the pS422 antibody, whereas tau truncation at aspartate 421 by caspase 3 (Asp421) and detected with a Tau C3 antibody occurs later during NFT formation [37]. A recent report identified conformational changes such as exposure of an amino-terminal motif and oligomerization as a very early pathological modification in the AD [44–46] and CTE [44] brain. While the involvement of p-tau containing NFTs within nbM neurons has been identified as a pathological lesion in CTE [9, 11, 47], to our knowledge there have been no studies investigating the progression of NFT pathology within the cholinergic neurons within the nbM in the CTE brain. The present study used site-specific tau antibodies to characterize NFT evolution in the cholinergic nbM neurons in tissue obtained at autopsy from former athletes and veterans exposed to repetitive mild TBI who were diagnosed neuropathologically with CTE using NINDS criteria [48] [9] [6, 11].

Methods

Subjects

A total of 18 brains were obtained from former male American professional and college football and hockey players and boxers, including two who were also military veterans (see Table 1). Institutional review board approval for brain donation was obtained through the Boston University Alzheimer's Disease Center (BUADC), CTE program and the Bedford VA hospital. Institutional Review Board approval for post-mortem clinical record review, interviews with family members and neuropathological analysis was obtained through Boston University School of Medicine.

Clinical evaluation

Clinical evaluation was performed according to the recent guidelines described by Mez and colleagues [49]. Briefly, a retrospective clinical evaluation was performed to obtain subject demographics including repetitive head injury exposure, substance use, medical, social and family histories. This evaluation is made up of a combination of online surveys and telephone calls between research personnel and family members as well as close friends of the individual. The collection of data is accomplished using an unstructured interview with either a behavioral neurologist or neuropsychologist (for details see [49]). Researchers performing the tests are blinded to the pathological examinations.

Neuropathological evaluation

BUADC Brain Bank performed the neuropathological staging of CTE as previously described [50] [9] [11]. Briefly, paraffin-embedded sections were processed histologically with Luxol fast blue, haematoxylin and eosin, and Bielschowsky's silver staining, and immunohistochemically using antibodies against phosphorylated tau (p-tau; AT8; Pierce Endogen, Rockford IL; 1:2,000), alpha-synuclein (rabbit polyclonal, Chemicon, Temecula, CA.; 1:15,000), amyloid-β (Aβ; 6F/3D; Dako North America, Inc.; 1:2,000), TDP-43 (Abcam; 1:1,000), phosphorylated TDP-43 (pTDP-43; pS409/410 mouse monoclonal;

Cosmo Bio Co, Tokyo, Japan; 1:2,000), and the phosphorylated neurofilaments, SMI-31 and SMI-34 (1:000, Sternberger Monoclonals, Inc) as previously described [7]. Neuropathological diagnosis was made blinded to the individual's clinical history and confirmed by two board certified neuropathologists. Following neuropathological staging, the paraffin blocks containing the nbM were shipped to Barrow Neurological Institute (Phoenix), where additional sections were collected for use in the present study.

Immunohistochemistry of the basal forebrain

Sections from a total of 18 cases containing the nbM and an additional 7 cases containing the vertical limb of the diagonal band of Broca (VDB) were immunohistochemically evaluated. However, only the cases containing nbM were used for quantitation and are included in Table 1. .Sections were slide mounted, deparaffinized, rehydrated and boiled in a citric acid solution (pH 6) for 5 minutes. Sections were immunostained with either a goat polyclonal antibody against choline acetyltransferase (ChAT; dilution 1:500; Millipore, MA), a mouse monoclonal antibody against human $p75^{NTR}$ (1:500; Thermo Scientific, Waltham, MA), a rabbit polyclonal antibody against the phospho-tau epitope pS422 (1:500; Thermo Fisher Scientific Pierce, Rockford, IL) [42, 51], a mouse monoclonal antibody against the tau Asp421 cleavage neoepitope, Tau C3 (1:50, dilution; Thermo Scientific, Waltham, MA) [37, 52] [35], a mouse monoclonal TOC1 (tau oligomeric complex 1) antibody (1:500; a gift from the late Dr. Lester "Skip" Binder) that is selective for non-fibrillar tau oligomers [53] [54] and a mouse monoclonal antibody TNT1 antibody (1:3000; a gift from Dr. Lester "Skip" Binder) that recognizes the phosphatase activating domain (PAD) region of tau, which is involved in the inhibition of anterograde, kinesin-based fast axonal transport (FAT) by activating axonal protein phosphatase 1 (PP1) and glycogen synthase kinase 3 (GSK3) [55] and the rabbit polyclonal antibody against the autophage marker p62 or SQSTM1 (1:500 dilution; Thermo Fisher Scientific Pierce, Rockford, IL) in a 0.1 M TBS/1% normal goat or horse serum solution overnight at 4°C. Additional sections were stained for Aβ and TDP-43 using the 6E10 monoclonal antibody (1:1000; Covance, Princeton, NJ) that recognizes both the Aβ precursor protein (APP) and Aβ [56, 57] and the rabbit polyclonal anti TAR-DNA binding protein-43 (TDP-43) (1:5000; Proteintech Group, Chicago, IL), respectively. Sections stained for TDP-43 and APP/Aβ were processed for antigen retrieval using Target Antigen Retrieval Solution, pH 9.0 (DAKO, Carpinteria, CA) for 20 min in a steamer [58] and 88% formic acid for 7 minutes, respectively. Sections were incubated in 0.1M Tris-buffered saline (TBS, pH 7.4) containing 0.1 M sodium periodate to eliminate endogenous peroxidase activity, blocked with 0.1 M TBS containing 0.25% Triton X-100 and 10% normal goat serum (NGS; Vector Labs, Burlingame, CA) for 1 hour. Sections were then incubated with biotinylated goat anti-mouse IgG (1:500; Vector Labs, Burlingame, CA), goat or horse anti-rabbit (1:200, Vector Labs) and horse anti-goat (1:200; Vector Labs), and processed with avidin-biotin complex reagent (ABC; Vector Labs, Burlingame, CA). Tissue was then developed in 0.05% 3', 3'-diaminobenzidine (DAB) and 0.005% H_2O_2 resulting in a brown reaction product. Slides were dehydrated in a series of graded concentrations of ethanol (70, 90, 95, and 100%), cleared in xylenes and cover-slipped using DPX (Electron Microscopy sciences, Hatfield, PA). Select sections were counterstained with cresyl violet for cytoarchitectural analysis.

Dual Immunohistochemistry

A second series of sections were dual-immuostained with either a rabbit (1:250; Millipore, MA) or a mouse (1:500; Thermo Scientific) anti human $p75^{NTR}$ antibody, a well-established marker for human CBF neurons [59–61], and each tau antibodies (pS422, TOC1, or TNT1). Due to methodological difficulties were unable to dual labeling in tissue from each case using the rabbit polyclonal $p75^{NTR}$antibody and the monoclonal TOC1 and TNT1 antibodies making it difficult to accurately quantitative double stained neurons in these experiments. Therefore our dual neuronal quantitation was performed only on sections concurrently stained with the mouse monoclonal $p75^{NTR}$ and pS422 antibodies. After visualizing $p75^{NTR}$ (as described above), tissue was incubated with an avidin/biotin blocking kit (Vector Laboratories, Burlingame, CA) and any remaining peroxidase activity was quenched with 3% H_2O_2 for 30 minutes at room temperature. Blocking buffer was reapplied for 1 hour at room temperature and the tissue was incubated in the second primary antibody (pS422, TOC1, or TNT1) overnight at 4°C and next day for 1 hour at room temperature before incubation with the appropriate biotinylated secondary antibody (1:500 in dilution buffer, Vector Laboratories, Burlingame, CA) for 2 hours at room temperature. Tissues were then incubated in ABC solution as described above. Sections were processed with the Vector SG Substrate Kit (blue reaction product, Vector Laboratories, Burlingame, CA) according to the manufacturer's protocol. This dual staining resulted in an easily identifiable two-colored profile: brown for $p75^{NTR}$ and dark blue/black for pS422, TOC1 and TNT1 positive profiles. Slides were air-dried, dehydrated, cleared in xylenes and cover-slipped.

Omission of primary antibodies resulted in no detectable immunostaining (not shown). AD basal forebrain tissue was processed in parallel with CTE tissue as a positive control for each antibody and to compare the morphological characteristics of NFT pathology between the two disorders (see Fig. 1).

Immunofluorescence and histofluorescence

To examine the fibrillar nature of NFTs within cholinergic neurons, sections were double stained for $p75^{NTR}$ and X-34, a highly fluorescent derivative of Congo Red, which detects the full spectrum of AD amyloid pathology with greater sensitivity than thioflavin S [62, 63]. The pan-amyloid dye X-34 is a highly fluorescent derivative of Congo red; it labels β-sheet structure of Aβ fibrils in plaques as well as tau fibrils in NFT, dystrophic neurites, and neuropil threads [63]. Briefly, sections were deparaffinized, rehydrated and treated with Protease XXIV (Sigma, MO) for 5 min at 37 °C and washed in potassium phosphate buffer (KPBS, pH 7.4). To reduce autofluorescence, sections were incubated in 0.25% $KMnO_4$ in KPBS for 20 min, rinsed in KPBS and incubated in 1% potassium meta-bisulfite and oxalic acid for 5 min at room temperature. Subsequently, slides were washed in Tris buffered saline (TBS, pH 7.4), followed by several rinses in TBS/0.25% Triton X-100 (TTBS) and incubated in a 3% goat serum/ TBS Triton X-100 blocking solution for 1 hour at room. Tissue was then incubated with mouse anti-$p75^{NTR}$ (1:50 dilution; Thermo Scientific, Waltham, MA) in TTBS/1% goat serum overnight at 4°C, followed by goat anti-mouse AlexaFluor 594 secondary antibody (1:200; Jackson ImmunoResearch Lab, West Grove, PA) at room temperature for 1 hour. After several washes in TBS and KPBS, sections were then incubated in 100μM X-34 [63] for 10 min at room temperature followed by a brief

wash in tap water and incubation in 80% ethanol for 2 min at room temperature. Sections were then rinsed in running tap water for 10 min and cover-slipped with Fluoromount-G (Southern Biotech, Birmingham, AL). Stains were imaged using an Olympus BX53 microscope with an X-Cite 120Q fluorescence attachment. Immunofluorescence $p75^{NTR}$ profiles were detected using the TRITC filter and X-34 was detected using an ultraviolet filter set. Single $p75^{NTR}$ and X-34 images were merged using the Layer blend option in Photoshop 6.0.

Quantitation of NFT profiles within the nbM

Counts of double pS422/$p75^{NTR}$ and single $p75^{NTR}$, TOC1, TNT1, Tau C3 and p62 positive neurons were performed within two sections representing the extent of the nbM in each case, using the Nikon Microphot-FXA microscope at 10x magnification. For each antibody, counts of all p-tau labeled neurons were averaged per case [57] and normalized to the total number of $p75^{NTR}$ positive neurons. Results are presented as percentage of cell counts. Fiduciary landmarks were used to prevent repetitive counting of labeled profiles.

Statistical Analysis

Demographic and clinical characteristics as well as cell counts were evaluated across pathological CTE stages II, III and IV using a one-way analysis of variance, Kruskal-Wallis test followed by Holm-Sidak and Dunn's post hoc test for multiple comparisons as appropriate, and Spearman rank for correlations (Sigma Plot 12.5, Systat Software, San Jose, CA). Statistical significance was set at 0.05 (two-tailed).

Results

Case demographics

Table 1 shows the demographics of the 18 male cases with a history of repetitive mild TBI. Cases were categorized as CTE Stage II, III, or IV according to the criteria published by McKee and colleagues [9] [11]. Stage II cases (n=7; mean age 41.9±19.2) included three National football players, one semi-professional American football player, one American college football player, one high school football/wrestler/pole vaulter and one professional hockey player. Stage III cases (n=5; mean age 54.8.9±9.3) were all National football league football players. Stage IV cases (n=6; mean age 75.0±6.8) included five National football league players, of which two were also military veterans, and a professional boxer. The groups differed by age (p=0.002), with stage IV cases significantly older compared to stage II, but no differences were found when compared by age to the time at which sport begun, years of play, age at symptom onset, time interval between retirement and symptom onset, and interval between symptom onset and death (Table 2).

Older age when sport begun was associated with older age at symptoms onset (r=0.60, p<0.008), longer interval between symptoms onset and death (r=0.48, p<0.04), and with older age at death (r=0.72, p<0.0003) (Table 3). Older age at symptoms onset was also associated with longer interval between symptoms onset and retirement from sport (r=0.85, p<0.00001), and with older age at death (r=0.71, p=0.0005). In addition, older age at death

was associated with longer intervals from symptom onset to either retirement from sport (r=0.52, p=0.02) or death (r=0.64, p=0.003) (Table 3).

Pathological findings

Consistent with previous reports [13] [64], other pathologies were present in the subjects with CTE: 13/18 (72%) had pTDP-43 inclusions; 6/18 (33%) had diffuse Aβ plaques; 3/18 (17%) had neuritic Aβ plaques; and 1/18 (6%) had Lewy body disease. Co-morbid pathologies were more common in older subjects with CTE with a higher CTE stage.

Tau pathology within the nbM and VDB

Nissl stained sections revealed clusters of large hyperchromic magnocellular neurons within the nbM extending anteriorly at the level of the crossing of the anterior commissure to the emergence of the commissure at the level of the amygdala (Fig. 1A–C1). In seven cases, the VDB was included in the paraffin block, however, this area was not included in the primary analysis (Fig. 1D–E). The phenotype of the cholinergic neurons was determined using either an antibody against ChAT or $p75^{NTR}$, accepted markers for cholinergic neurons in the human basal forebrain [65]. In agreement with a previous report [22], we were unable to consistently visualize ChAT positive neurons within the nbM (Fig.1F) across the cases examined, most likely due to antibody fixation interactions. Therefore, quantitative and qualitative analysis were performed using the $p75^{NTR}$ antibody (Fig. 1G). For all cases, a section containing the nbM from an AD case was included as a positive control for each tau antibody (Fig. 1H–M). pS422, TOC1, TNT1, Tau C3 and p62 positive neurons were globose in appearance as seen in the nbM in AD [66]. Qualitative analysis revealed that there were more pS422-ir profiles (Fig. 1G) compared to oligomeric TOC1 (Fig. 1J), TNT1 (Fig. 1K), Tau C3 (Fig. 1L) and p62 (Fig. 1M) profiles in the nbM similar to our AD studies [13].

In CTE cases, mainly in stages III and IV, many $p75^{NTR}$ positive neurons appeared globose in shape indicative of tangle bearing neurons [13, 67]; this was confirmed in adjacent sections immunostained with pS422 (Fig. 2A–I), oligomeric TOC1 (Fig. 2J–N), TNT1 (Fig. 2O–S) and TauC3 (Fig. 3A–C). Numbers of TOC1, TNT1, pS422, Tau C3 and p62 positive nbM neurons increased with more advanced CTE stage (Figs. 2A–Q and 3A–F). Dual $p75^{NTR}$ and pS422 immunostaining revealed co-labeled as well as single $p75^{NTR}$ and pS422 neurons within the nbM at each CTE stage (Fig. 2A–C). At any CTE stage, the greatest number of tau positive neurons, was observed using the pS422 antibody (Table 4, Fig. 2A–C). In stage III and IV cholinergic neurons display granular pS422 staining suggestive of an early stage of tangle development (Fig. 2D, E). Both $p75^{NTR}$/pS422 (Fig. 2F, G) and single pS422 (Fig. 2H, I) containing neurons displayed twisted tau filamentous resembling skeins of yarn [68] indicative of cellular degeneration [33]. The same morphological changes in the nbM cholinergic neurons were observed using the other tau markers (Fig. 2M, N, R, and S). Likewise, the greatest extent of immunoreactive neurites in the nbM was seen in stage IV, using pS422 (Fig. 2C) and TOC1 (Fig. 2L) antibodies, followed by TNT1 (Fig. 2R) and to a lesser degree Tau C3 (Fig. 3C) and p62 (Fig. 3F). We also observed pS422, TOC1 and TNT1 positive astrocytes surrounding large blood vessels within the nbM, mainly in stages III and IV (Fig. 3G–I). Similar NFT pathology was seen in the VDB in stage III and IV (Fig. 1D and E).

Quantitative analysis revealed that more advanced CTE pathological stage was associated with increased numbers of neurons positive for all tau markers and for p62 within the nbM (Table 4 and Fig. 4). Percent of double pS422/p75, and single pS422, and TOC1 and TNT1 positive nbM neurons was significantly different among the three CTE stages ($p<0.01$ for all markers) with stage IV greater than stage II but not stage III (Table 4). The three CTE groups also differed by the number of Tau C3 ($p=0.009$) and p62 ($p=0.002$) positive neurons, with stages III and IV greater than stage II (Table 4). Approximately 50% of all pS422 neurons were $p75^{NTR}$ dual stained across all stages (Table 4).

Dual histofluorescence for fibrillar tau in the nbM

Double fluorescence analysis revealed that $p75^{NTR}$-immunoreactive nbM neurons contained NFT-like X-34 positive tau fibrils in stages III and IV, and to a lesser extent in stage II (Fig. 5A–F). In stage III and IV, most of the NFTs were singled stained for X-34 (Fig. 5D–F). X-34 positive plaques were not seen in the nbM at any CTE stage. However, in two of the 18 cases examined X-34 positive plaques were seen in the insular cortex.

Aβ immunostaining in the nbM

To determine the involvement of beta amyloid in the nbM in CTE, sections were immunostained using the 6E10 monoclonal antibody. We observed only diffuse, but not cored Aβ plaques and vascular Aβ deposits in the nbM in five stage IV CTE cases (Fig. 5G–I). Intracellular Aβ/APP immunoreactivity was not seen in nbM neurons in any of the CTE cases examined (Fig. 5G, H). By contrast, both diffuse and cored/neuritic Aβ/APP plaques and vascular amyloid deposits were found in the insula, anterior temporal cortex as well as and striatum in all stage IV CTE cases examined (Fig. 5I, J).

TDP43 immunostaining in the nbM

To examine whether TDP-43 was involved in the pathology of nbM neurons, sections were immunostained using a TDP-43 antibody, which reveals intact and post-transcriptional changes in this primarily nuclear protein. In addition to the non-pathological nuclear TDP-43-ir in CTE nbM neurons, lenticular shaped TPD-43-ir inclusions (Fig. 5K–L) were observed within nbM neurons in CTE but not in the AD basal forebrain (Fig. 5M).

Correlations between percentage of NFTs in the nbM and demographics

Across all CTE stages, there was a strong statistically significant association among the pS422/$p75^{NTR}$, pS422, TOC1, TNT1, Tau C3 and p62 positive neurons (Table 5). A greater percent of pS422/$p75^{NTR}$, pS422 and TNT1 labeled neurons were significantly c orrelated with age at symptom onset (Fig. 6A–C) (pS422/$p75^{NTR}$: $r= 0.053$, $p= 0.02$; pS422: $r= 0.049$, $p= 0.03$; TNT1, $r= 0.50$, $p= 0.04$), interval between symptom onset and death (pS422/$p75^{NTR}$: $r= 0.061$, $p= 0.006$; pS422: $r= 0.62$, $p= 0.005$; TNT1, $r= 0.54$, $p= 0.02$, respectively) and age at death (Fig. 6D–F) (pS422/$p75^{NTR}$: $r= 0.075$, $p= 0.00007$; pS422: $r= 0.73$, $p= 0.0003$; TNT1, $r= 0.67$, $p= 0.002$) (Table 6). Greater percent of TOC1, TauC3 and p62-ir nbM neurons were significantly associated with longer intervals between symptom onset (TOC1: $r= 0.62$, $p= 0.05$; Tau C3: $r= 0.67$, $p= 0.002$; p62: $r= 0.68$, $p=0.002$) and older

age at death (TOC1: r= 0.65, p=0.003; Tau C3: r= 0.65, p= 0.004; p62: r= 0.51, p= 0.03) (Table 6).

Discussion

The present findings demonstrate that cholinergic nbM neurons develop progressive NFT pathology in CTE similar to the changes with p-tau-positive neurofibrillary pathology seen in prodromal and frank AD [17]. These finding support the concept that cortical projecting neurons belonging to cholinergic and likely other neurotransmitter systems (i.e., locus coereulus noradrenergic neurons [69]) are vulnerable following CTE. Moreover, cholinergic mbM neurons in CTE develop NFT within nbM neurons in a sequence characterized by the appearance of the pretangle marker phospho-tau epitope pS422, oligomeric tau (TOC1) and Tau C3, a late stage apoptotic marker, similar to that found in AD [66]. These results confirm previous reports of NFTs within the nbM [9] and support findings showing these specific forms of p-tau pathology in the frontal cortex of individuals with CTE [44]. Here we also report that the nbM like frontal cortex neurons [44] are immunoreactive to TNT1, another pretangle antibody that recognizes the phosphatase activating domain (PAD) region of tau, involved in the inhibition of anterograde, kinesin-based fast axonal transport (FAT) by activating axonal protein phosphatase 1 (PP1) and glycogen synthase kinase 3 (GSK3) [55]. We observed significantly greater numbers of TOC1, TNT1 and pS422 positive neurons in stage IV compared to stage II but not stage III, which may be due to the single stage III case that displayed NFT counts similar to that seen in stage IV. There was also a significantly greater number of Tau C3 and p62 positive neurons in stages III and IV compared to stage II. The expression of p62 positive neurons across all pathological stages of CTE suggests that cholinergic nbM neurons undergo autophagic as well as cytoskeletal alterations in CTE. The display of p62 suggests that these neurons are experiencing problems related to clearance of cellular debris due to a breakdown of autophagic mechanism similar to that seen in AD [70–72]. Across CTE stages we observed dual labeled $p75^{NTR}$/pS422 but also single $p75^{NTR}$ and pS422 labeled neurons within the nbM. Compared to stage II, cases classified as stage IV, had significantly more $p75^{NTR}$ neurons co-labeled with pS422. These finding indicate that nbM neurons develop NFTs gradually across the pathological stages of CTE. It remains to be determined whether NFT changes are present in nbM neurons at the very onset of pathological CTE (e.g. stage I). Regardless, the present data indicate that development of pre-tangle changes in the cholinergic nbM neurons may contribute to cholinergic dysfunction [66] and play a role in the onset of cognitive impairment in CTE [21] [73]. The protracted development of NFTs within the cholinergic neurons of the nbM may coincide with the presymptomatic period between the exposure to head trauma and the onset of clinical symptoms in CTE, and may mark a window of opportunity for therapies.

The present finding of NFT pathology progression within cholinergic nbM neurons may underlie the observation that ChAT activity in the inferior temporal [74], cingulate and parietal cortex [22] each of which are innervated by select cholinergic subfields of the nbM is significantly reduced in TBI [18]. Despite the loss of cholinergic activity in the cortex of CTE, postsynaptic cholinergic receptors including muscarinic [74] and nicotinic ($\alpha_4\beta_2$ and $\alpha 7$) [75] subtypes are preserved, indicating that cholinergic therapies are feasible in subjects surviving CTE. During the past several years a group of drugs targeting the reuptake of Ach

at the synapse have been used to treat mild to moderate AD [76–81], and several of these drugs have been identified as a treatment option for patients with TBI [4] [21]. Donepezil, a centrally acting AChE inhibitor, has been shown to improve cognitive function and attention in TBI patients [25] [82] [83]. On the other hand, several studies reported no significant change in cognitive function after Donepezil treatment of TBI [26, 27] [28]. Interestingly, a study suggested that Donepezil administration may be beneficial early following TBI [27]. Since formation of NFTs within the nbM is an early event and continues progressively during the pathological course of CTE, therapies preventing the build-up of p-tau within cholinergic nbM cortical and hippocampal projection neurons could represent a therapeutic target for CTE, similar to AD.

A proportion of subjects with CTE have both tau pathology and Aβ plaques, and a subset also meet the pathological criteria for AD [84]. In a study of a heterogeneous cohort of deceased CTE cases diffuse or neuritic amyloid plaques were seen in the cortex in just over half of the subjects [84], a finding also confirmed in the present report. However, we found that even at advanced stages of CTE (stage IV) with neocortical neuritic Aβ plaques, the nbM contains only diffuse plaques. It has been suggested that in AD, cortical plaque pathology can initiate a retrograde cellular response within these cholinergic neurons [85] that triggers tau overexpression and results in neuronal degeneration and cholinergic dysfunction. Whether a similar cortical process plays a role in NFT formation in cholinergic nbM neurons in subjects with CTE remains to be explored.

Here we found that the percent of pS422, TOC1, TNT1, Tau C3 and p62-ir nbM neurons are highly correlated across all pathological stages of CTE. These findings compliment a biochemical study showing changes in soluble and insoluble tau fractions within the frontal cortex of CTE cases [44], suggesting that pS422, PAD exposure and tau oligomerization occur across brain regions. Interestingly, a correlation between the biochemical levels of Tau C3 was not found in the frontal cortex suggesting that there may be some tau changes that are regionally specific in CTE [44] or that the analysis of total brain tissue for biochemistry include non-neuronal profiles (i.e., p-tau positive glia). Our findings are also similar to the sequence of tau biochemical [66] and intraneuronal cytoskeletal changes seen in AD [33]. Here, we observed pS422, TNT1 and TOC1 astrocytic pathology in the nbM suggesting that the tau pathology in both, neurons and glial undergo similar modifications in this region. In fact, glia positive for these tau markers were shown within astrocytes, but not microglia, in CTE frontal cortex [44]. Importantly, pS422 containing tangles has been shown to be the strongest correlate of cognitive impairment in AD [66]. Whether a similar association exists in CTE remains to be investigated, although CTE stage correlates with the progression of clinical symptoms [9].

We observed that greater numbers of pretangle neurons positive for pS422 and TNT1 (a marker of neuronal anterograde axonal transport defect) as well as for TOC1 and Tau C3 were associated significantly with older age at symptom onset, longer interval between symptom onset and death, and older age at death, suggesting their potential biomarker value for the pathological progression of CTE. Our findings suggest that the pathobiological evolution of p-tau positive NFTs within the nbM as well as in the frontal cortex [44] may contribute to cognitive symptoms in CTE. Diffuse axonal damage due to acceleration/

deceleration head injuries results in axonal tearing or at a minimum disruption in axonal transport and it is possible that axonal damage in CTE involves impaired axonal transport leading to p-tau accumulation and NFT formation [86] as suggested in AD [17]. We found abnormal TDP-43 nuclear inclusions in nbM neurons during the pathological progression of CTE stage supporting earlier reports of these inclusions in cortical neurons in TBI/CTE cases [87]. Whether the TDP-43 inclusions seen within the nbM neurons effect gene transcription, RNA transcription, preRNA splicing or mRNA biogenesis in these neurons remain unknown.

Moreover, there are several limitations to the findings presented in this study. We examined a limited autopsy cohort containing a heterogeneous population of subjects with a history of CTE. Therefore, the cases examined here may not be representative of the larger CTE population. In addition, the clinical histories were obtained retrospectively from family members and thus they may be subject to bias. Future prospective clinical and pathological investigations are needed to determine the interaction between cholinergic and other pathologies with cognitive impairment in subjects with CTE.

In summary, the present study provides evidence that the cholinergic nbM neurons are affected with NFT pathology early following a progression of tau epitope during the pathological stages of CTE. This progression of NFT pathology follows a linear model, which can be observed by antibodies directed against p-tau epitopes marking early, intermediate, and late stages of NFT development similar to that seen during the progression of AD [37–42]. We also found in the nbM of advanced CTE cases that the coexistence of Aβ pathology, when present, was restricted to diffuse and vascular Aβ deposits. Although neuritic Aβ plaques were absent from the nbM in all CTE cases examined, this type of Aβ pathology was seen in adjacent cortex. TDP-43 abnormal inclusions were also seen early in the pathological staging of subjects with CTE. The involvement of these lesions in the onset of dementia in CTE remains to be determined. Further studies are needed to determine the mechanisms driving the formation of NFTs and TDP-43 inclusions within the nbM and their interaction with other alterations that are also seen in AD [67].

Acknowledgments

The authors gratefully acknowledge the use of the resources and facilities at the Edith Nourse Rogers Memorial Veterans Hospital (Bedford, MA, USA). We thank Ms. L. Shao and Ms. Diana Waters for technical assistance and Dr. William Klunk (University of Pittsburgh) for providing X-34.

This material is based upon work supported by the U.S. Army Medical Research and Material Command and from the U.S. Department of Veterans Affairs [2] under Award No. W81XWH-13-2-0095. The U.S. Army Medical Research Acquisition Activity, 820 Chandler Street, Fort Detrick MD 21702-5014 is the awarding and administering acquisition office. Any opinions, findings, conclusions or recommendations expressed in this publication are those of the author(s) and do not necessarily reflect the views of the U.S. Government, or the U.S. Department of Veterans Affairs, and no official endorsement should be inferred. This work was also supported by an award from the Department of Veterans Affairs No. I01 RX001774, National Institute of Neurological Disorders and Stroke, National Institute of Biomedical Imaging and Bioengineering (U01NS086659-01) and National Institute of Aging Boston University AD Center (P30AG13846; supplement 0572063345-5), the Veterans Affairs Biorepository (CSP 501, the National Operating Committee on Standards for Athletic Equipment, the Concussion Legacy Foundation, the Andlinger Foundation and the World Wrestling Entertainment and the National Football League.

References

1. Cifu DX, Taylor BC, Carne WF, Bidelspach D, Sayer NA, Scholten J, Campbell EH. Traumatic brain injury, posttraumatic stress disorder, and pain diagnoses in OIF/OEF/OND Veterans. J Rehabil Res Dev. 2013; 50:1169–1176. [PubMed: 24458958]
2. David X Cifu D-AR, Williams RL, Carne W, West SL, McDougal M, Dixon K. Chronic Effects of Neurotrauma Consortium: An Overview at Year 1. Fed Pract. 2015; 32:44–48.
3. Shively S, Scher AI, Perl DP, Diaz-Arrastia R. Dementia resulting from traumatic brain injury: what is the pathology? Arch Neurol. 2012; 69:1245–1251. [PubMed: 22776913]
4. Shin SS, Dixon CE. Alterations in Cholinergic Pathways and Therapeutic Strategies Targeting Cholinergic System after Traumatic Brain Injury. J Neurotrauma. 2015; 32:1429–1440. [PubMed: 25646580]
5. Omalu B, Hammers JL, Bailes J, Hamilton RL, Kamboh MI, Webster G, Fitzsimmons RP. Chronic traumatic encephalopathy in an Iraqi war veteran with posttraumatic stress disorder who committed suicide. Neurosurg Focus. 2011; 31:E3.
6. McKee AC, Daneshvar DH, Alvarez VE, Stein TD. The neuropathology of sport. Acta Neuropathol. 2014; 127:29–51. [PubMed: 24366527]
7. McKee AC, Cantu RC, Nowinski CJ, Hedley-Whyte ET, Gavett BE, Budson AE, Santini VE, Lee HS, Kubilus CA, Stern RA. Chronic traumatic encephalopathy in athletes: progressive tauopathy after repetitive head injury. J Neuropathol Exp Neurol. 2009; 68:709–735. [PubMed: 19535999]
8. Goldstein LE, Fisher AM, Tagge CA, Zhang XL, Velisek L, Sullivan JA, Upreti C, Kracht JM, Ericsson M, Wojnarowicz MW, et al. Chronic traumatic encephalopathy in blast-exposed military veterans and a blast neurotrauma mouse model. Sci Transl Med. 2012; 4:134ra160.
9. McKee AC, Stern RA, Nowinski CJ, Stein TD, Alvarez VE, Daneshvar DH, Lee HS, Wojtowicz SM, Hall G, Baugh CM, et al. The spectrum of disease in chronic traumatic encephalopathy. Brain. 2013; 136:43–64. [PubMed: 23208308]
10. McKee AC, Robinson ME. Military-related traumatic brain injury and neurodegeneration. Alzheimers Dement. 2014; 10:S242–S253. [PubMed: 24924675]
11. McKee AC, Stein TD, Kiernan PT, Alvarez VE. The neuropathology of chronic traumatic encephalopathy. Brain Pathol. 2015; 25:350–364. [PubMed: 25904048]
12. Daneshvar DH, Goldstein LE, Kiernan PT, Stein TD, McKee AC. Post-traumatic neurodegeneration and chronic traumatic encephalopathy. Mol Cell Neurosci. 2015; 66:81–90. [PubMed: 25758552]
13. Vana L, Kanaan NM, Ugwu IC, Wuu J, Mufson EJ, Binder LI. Progression of tau pathology in cholinergic Basal forebrain neurons in mild cognitive impairment and Alzheimer's disease. The American journal of pathology. 2011; 179:2533–2550. [PubMed: 21945902]
14. Stein TD, Alvarez VE, McKee AC. Chronic traumatic encephalopathy: a spectrum of neuropathological changes following repetitive brain trauma in athletes and military personnel. Alzheimers Res Ther. 2014; 6:4. [PubMed: 24423082]
15. Mesulam M. Cholinergic aspects of aging and Alzheimer's disease. Biological psychiatry. 2012; 71:760–761. [PubMed: 22482884]
16. Mufson EJ, Counts SE, Perez SE, Ginsberg SD. Cholinergic system during the progression of Alzheimer's disease: therapeutic implications. Expert review of neurotherapeutics. 2008; 8:1703–1718. [PubMed: 18986241]
17. Mufson EJ, Binder L, Counts SE, DeKosky ST, de Toledo-Morrell L, Ginsberg SD, Ikonomovic MD, Perez SE, Scheff SW. Mild cognitive impairment: pathology and mechanisms. Acta neuropathologica. 2012; 123:13–30. [PubMed: 22101321]
18. Mesulam MM, Mufson EJ, Levey AI, Wainer BH. Cholinergic innervation of cortex by the basal forebrain: cytochemistry and cortical connections of the septal area, diagonal band nuclei, nucleus basalis (substantia innominata), and hypothalamus in the rhesus monkey. J Comp Neurol. 1983; 214:170–197. [PubMed: 6841683]
19. Whitehouse PJ, Price DL, Struble RG, Clark AW, Coyle JT, Delon MR. Alzheimer's disease and senile dementia: loss of neurons in the basal forebrain. Science. 1982; 215:1237–1239. [PubMed: 7058341]

20. DeKosky ST, Ikonomovic MD, Styren SD, Beckett L, Wisniewski S, Bennett DA, Cochran EJ, Kordower JH, Mufson EJ. Upregulation of choline acetyltransferase activity in hippocampus and frontal cortex of elderly subjects with mild cognitive impairment. Ann Neurol. 2002; 51:145–155. [PubMed: 11835370]
21. Arciniegas DB. The cholinergic hypothesis of cognitive impairment caused by traumatic brain injury. Curr Psychiatry Rep. 2003; 5:391–399. [PubMed: 13678561]
22. Murdoch I, Nicoll JA, Graham DI, Dewar D. Nucleus basalis of Meynert pathology in the human brain after fatal head injury. J Neurotrauma. 2002; 19:279–284. [PubMed: 11898797]
23. Pike BR, Hamm RJ. Activating the posttraumatic cholinergic system for the treatment of cognitive impairment following traumatic brain injury. Pharmacol Biochem Behav. 1997; 57:785–791. [PubMed: 9259007]
24. Donat CK, Walter B, Deuther-Conrad W, Wenzel B, Nieber K, Bauer R, Brust P. Alterations of cholinergic receptors and the vesicular acetylcholine transporter after lateral fluid percussion injury in newborn piglets. Neuropathol Appl Neurobiol. 2010; 36:225–236. [PubMed: 19889177]
25. Tenovuo O. Central acetylcholinesterase inhibitors in the treatment of chronic traumatic brain injury-clinical experience in 111 patients. Prog Neuropsychopharmacol Biol Psychiatry. 2005; 29:61–67. [PubMed: 15610946]
26. Masanic CA, Bayley MT, VanReekum R, Simard M. Open-label study of donepezil in traumatic brain injury. Arch Phys Med Rehabil. 2001; 82:896–901. [PubMed: 11441374]
27. Walker W, Seel R, Gibellato M, Lew H, Cornis-Pop M, Jena T, Silver T. The effects of Donepezil on traumatic brain injury acute rehabilitation outcomes. Brain Inj. 2004; 18:739–750. [PubMed: 15204315]
28. Kaye NS, Townsend JB 3rd, Ivins R. An open-label trial of donepezil (aricept) in the treatment of persons with mild traumatic brain injury. J Neuropsychiatry Clin Neurosci. 2003; 15:383–384. author reply 384-385. [PubMed: 12928519]
29. Hefti F. Is Alzheimer disease caused by lack of nerve growth factor? Ann Neurol. 1983; 13:109–110. [PubMed: 6830157]
30. Hefti F, Weiner WJ. Nerve growth factor and Alzheimer's disease. Annals of neurology. 1986; 20:275–281. [PubMed: 3532929]
31. Kaplan DR, Miller FD. Neurotrophin signal transduction in the nervous system. Curr Opin Neurobiol. 2000; 10:381–391. [PubMed: 10851172]
32. Teng KK, Hempstead BL. Neurotrophins and their receptors: signaling trios in complex biological systems. Cell Mol Life Sci. 2004; 61:35–48. [PubMed: 14704852]
33. Sassin I, Schultz C, Thal DR, Rub U, Arai K, Braak E, Braak H. Evolution of Alzheimer's disease-related cytoskeletal changes in the basal nucleus of Meynert. Acta Neuropathol. 2000; 100:259–269. [PubMed: 10965795]
34. Johnson GVW, Hartigan JA. Tau protein in normal and Alzheimer's disease brain: An update. Alzheimer's Disease Review. 1998; 3:125–141.
35. Buee L, Bussiere T, Buee-Scherrer V, Delacourte A, Hof PR. Tau protein isoforms, phosphorylation and the role in neurodegenerative disorders. Brain Res Brain Res Rev. 2000; 33:95–130. [PubMed: 10967355]
36. Mesulam M, Shaw P, Mash D, Weintraub S. Cholinergic nucleus basalis tauopathy emerges early in the aging-MCI-AD continuum. Ann Neurol. 2004; 55:815–828. [PubMed: 15174015]
37. Guillozet-Bongaarts AL, Garcia-Sierra F, Reynolds MR, Horowitz PM, Fu Y, Wang T, Cahill ME, Bigio EH, Berry RW, Binder LI. Tau truncation during neurofibrillary tangle evolution in Alzheimer's disease. Neurobiol Aging. 2005; 26:1015–1022. [PubMed: 15748781]
38. Ghoshal N, Garcia-Sierra F, Fu Y, Beckett LA, Mufson EJ, Kuret J, Berry RW, Binder LI. Tau-66: evidence for a novel tau conformation in Alzheimer's disease. J Neurochem. 2001; 77:1372–1385. [PubMed: 11389188]
39. Ghoshal N, Garcia-Sierra F, Wuu J, Leurgans S, Bennett DA, Berry RW, Binder LI. Tau Conformational Changes Correspond to Impairments of Episodic Memory in Mild Cognitive Impairment and Alzheimer’s Disease. Exp Neurol. 2002; 177:475–493. [PubMed: 12429193]

40. Garcia-Sierra F, Ghoshal N, Quinn B, Berry RW, Binder LI. Conformational changes and truncation of tau protein during tangle evolution in Alzheimer's disease. J Alzheimer's Dis. 2003; 5:65–77. [PubMed: 12719624]
41. Binder LI, Guillozet-Bongaarts AL, Garcia-Sierra F, Berry RW. Tau, tangles, and Alzheimer's disease. Biochim Biophys Acta. 2005; 1739:216–223. [PubMed: 15615640]
42. Guillozet-Bongaarts AL, Cahill ME, Cryns VL, Reynolds MR, Berry RW, Binder LI. Pseudophosphorylation of tau at serine422 inhibits caspase cleavage: in vitro evidence and implications for tangle formation in vivo. Journal of Neurochemistry. 2006; 97:1005–1014. [PubMed: 16606369]
43. Garcia-Sierra F, Ghoshal N, Quinn B, Berry RW, Binder LI. Conformational changes and truncation of tau protein during tangle evolution in Alzheimer's disease. J Alzheimers Dis. 2003; 5:65–77. [PubMed: 12719624]
44. Kanaan NM, Cox K, Alvarez VE, Stein TD, Poncil S, McKee AC. Characterization of Early Pathological Tau Conformations and Phosphorylation in Chronic Traumatic Encephalopathy. J Neuropathol Exp Neurol. 2015
45. Patterson KR, Remmers C, Fu Y, Brooker S, Kanaan NM, Vana L, Ward S, Reyes JF, Philibert K, Glucksman MJ, Binder LI. Characterization of prefibrillar Tau oligomers in vitro and in Alzheimer disease. The Journal of biological chemistry. 2011; 286:23063–23076. [PubMed: 21550980]
46. Kanaan NM, Morfini GA, LaPointe NE, Pigino GF, Patterson KR, Song Y, Andreadis A, Fu Y, Brady ST, Binder LI. Pathogenic forms of tau inhibit kinesin-dependent axonal transport through a mechanism involving activation of axonal phosphotransferases. The Journal of neuroscience : the official journal of the Society for Neuroscience. 2011; 31:9858–9868. [PubMed: 21734277]
47. McKee AC, Daneshvar DH. The neuropathology of traumatic brain injury. Handb Clin Neurol. 2015; 127:45–66. [PubMed: 25702209]
48. McKee AC, Cairns NJ, Dickson DW, Folkerth RD, Keene CD, Litvan I, Perl DP, Stein TD, Vonsattel JP, Stewart W, et al. The first NINDS/NIBIB consensus meeting to define neuropathological criteria for the diagnosis of chronic traumatic encephalopathy. Acta Neuropathol. 2016; 131:75–86. [PubMed: 26667418]
49. Mez J, Solomon TM, Daneshvar DH, Murphy L, Kiernan PT, Montenigro PH, Kriegel J, Abdolmohammadi B, Fry B, Babcock KJ, et al. Assessing clinicopathological correlation in chronic traumatic encephalopathy: rationale and methods for the UNITE study. Alzheimers Res Ther. 2015; 7:62. [PubMed: 26455775]
50. Vonsattel JP, Aizawa H, Ge P, DiFiglia M, McKee AC, MacDonald M, Gusella JF, Landwehrmeyer GB, Bird ED, Richardson EP Jr, et al. An improved approach to prepare human brains for research. J Neuropathol Exp Neurol. 1995; 54:42–56. [PubMed: 7815079]
51. Guillozet-Bongaarts AL, Glajch KE, Libson EG, Cahill ME, Bigio E, Berry RW, Binder LI. Phosphorylation and cleavage of tau in non-AD tauopathies. Acta Neuropathologica. 2007; 113:513–520. [PubMed: 17357802]
52. Gamblin TC, Chen F, Zambrano A, Abraha A, Lagalwar S, Guillozet AL, Lu M, Fu Y, Garcia-Sierra F, LaPointe N, et al. Caspase cleavage of tau: linking amyloid and neurofibrillary tangles in Alzheimer's disease. Proc Natl Acad Sci U S A. 2003; 100:10032–10037. [PubMed: 12888622]
53. Patterson KR, Remmers C, Fu Y, Brooker S, Kanaan NM, Vana L, Ward S, Reyes JF, Philibert K, Glucksman MJ, Binder LI. Characterization of prefibrillar Tau oligomers in vitro and in Alzheimer disease. J Biol Chem. 2011; 286:23063–23076. [PubMed: 21550980]
54. Ward SM, Himmelstein DS, Lancia JK, Fu Y, Patterson KR, Binder LI. TOC1: characterization of a selective oligomeric tau antibody. J Alzheimers Dis. 2013; 37:593–602. [PubMed: 23979027]
55. Kanaan NM, Morfini GA, LaPointe NE, Pigino GF, Patterson KR, Song Y, Andreadis A, Fu Y, Brady ST, Binder LI. Pathogenic forms of tau inhibit kinesin-dependent axonal transport through a mechanism involving activation of axonal phosphotransferases. J Neurosci. 2011; 31:9858–9868. [PubMed: 21734277]
56. Perez SE, Lumayag S, Kovacs B, Mufson EJ, Xu S. Beta-amyloid deposition and functional impairment in the retina of the APPswe/PS1DeltaE9 transgenic mouse model of Alzheimer's disease. Invest Ophthalmol Vis Sci. 2009; 50:793–800. [PubMed: 18791173]

57. Perez SE, Nadeem M, Sadleir KR, Matras J, Kelley CM, Counts SE, Vassar R, Mufson EJ. Dimebon alters hippocampal amyloid pathology in 3xTg-AD mice. International journal of physiology, pathophysiology and pharmacology. 2012; 4:115–127.
58. Collins M, Riascos D, Kovalik T, An J, Krupa K, Krupa K, Hood BL, Conrads TP, Renton AE, Traynor BJ, Bowser R. The RNA-binding motif 45 (RBM45) protein accumulates in inclusion bodies in amyotrophic lateral sclerosis (ALS) and frontotemporal lobar degeneration with TDP-43 inclusions (FTLD-TDP) patients. Acta Neuropathol. 2012; 124:717–732. [PubMed: 22993125]
59. Schatteman GC, Gibbs L, Lanahan AA, Claude P, Bothwell M. Expression of NGF receptor in the developing and adult primate central nervous system. J Neurosci. 1988; 8:860–873. [PubMed: 2831315]
60. Kordower JH, Bartus RT, Bothwell M, Schatteman G, Gash DM. Nerve growth factor receptor immunoreactivity in the nonhuman primate (Cebus apella): distribution, morphology, and colocalization with cholinergic enzymes. J Comp Neurol. 1988; 277:465–486. [PubMed: 2850304]
61. Mufson EJ, Bothwell M, Kordower JH. Loss of nerve growth factor receptor-containing neurons in Alzheimer's disease: a quantitative analysis across subregions of the basal forebrain. Exp Neurol. 1989; 105:221–232. [PubMed: 2548888]
62. Styren SD, Hamilton RL, Styren GC, Klunk WE. X-34, a fluorescent derivative of Congo red: a novel histochemical stain for Alzheimer's disease pathology. The journal of histochemistry and cytochemistry : official journal of the Histochemistry Society. 2000; 48:1223–1232. [PubMed: 10950879]
63. Ikonomovic MD, Abrahamson EE, Isanski BA, Debnath ML, Mathis CA, Dekosky ST, Klunk WE. X-34 labeling of abnormal protein aggregates during the progression of Alzheimer's disease. Methods in enzymology. 2006; 412:123–144. [PubMed: 17046656]
64. Consensus recommendations for the postmortem diagnosis of Alzheimer's disease. The National Institute on Aging, and Reagan Institute Working Group on Diagnostic Criteria for the Neuropathological Assessment of Alzheimer's Disease. Neurobiol Aging. 1997; 18:S1–S2. [PubMed: 9330978]
65. Mufson EJ, Bothwell M, Hersh LB, Kordower JH. Nerve growth factor receptor immunoreactive profiles in the normal, aged human basal forebrain: colocalization with cholinergic neurons. The Journal of comparative neurology. 1989; 285:196–217. [PubMed: 2547849]
66. Vana L, Kanaan NM, Ugwu IC, Wuu J, Mufson EJ, Binder LI. Progression of tau pathology in cholinergic Basal forebrain neurons in mild cognitive impairment and Alzheimer's disease. Am J Pathol. 2011; 179:2533–2550. [PubMed: 21945902]
67. Mufson EJ, Binder L, Counts SE, DeKosky ST, de Toledo-Morrell L, Ginsberg SD, Ikonomovic MD, Perez SE, Scheff SW. Mild cognitive impairment: pathology and mechanisms. Acta Neuropathol. 2012; 123:13–30. [PubMed: 22101321]
68. E A. Memory Loss, Alzheimer's Disease, and Dementia. 2016
69. Omalu B, Bailes J, Hamilton RL, Kamboh MI, Hammers J, Case M, Fitzsimmons R. Emerging histomorphologic phenotypes of chronic traumatic encephalopathy in American athletes. Neurosurgery. 2011; 69:173–183. discussion 183. [PubMed: 21358359]
70. Boland B, Kumar A, Lee S, Platt FM, Wegiel J, Yu WH, Nixon RA. Autophagy induction and autophagosome clearance in neurons: relationship to autophagic pathology in Alzheimer's disease. J Neurosci. 2008; 28:6926–6937. [PubMed: 18596167]
71. Ginsberg SD, Mufson EJ, Alldred MJ, Counts SE, Wuu J, Nixon RA, Che S. Upregulation of select rab GTPases in cholinergic basal forebrain neurons in mild cognitive impairment and Alzheimer's disease. Journal of chemical neuroanatomy. 2011; 42:102–110. [PubMed: 21669283]
72. Nixon RA, Yang DS. Autophagy failure in Alzheimer's disease--locating the primary defect. Neurobiol Dis. 2011; 43:38–45. [PubMed: 21296668]
73. Stern RA, Daneshvar DH, Baugh CM, Seichepine DR, Montenigro PH, Riley DO, Fritts NG, Stamm JM, Robbins CA, McHale L, et al. Clinical presentation of chronic traumatic encephalopathy. Neurology. 2013; 81:1122–1129. [PubMed: 23966253]
74. Dewar D, Graham DI. Depletion of choline acetyltransferase activity but preservation of M1 and M2 muscarinic receptor binding sites in temporal cortex following head injury: a preliminary human postmortem study. J Neurotrauma. 1996; 13:181–187. [PubMed: 8860198]

75. Murdoch I, Perry EK, Court JA, Graham DI, Dewar D. Cortical cholinergic dysfunction after human head injury. J Neurotrauma. 1998; 15:295–305. [PubMed: 9605345]
76. Lopez-Pousa S, Vilalta-Franch J, Garre-Olmo J, Turon-Estrada A, Hernandez-Ferrandiz M, Cruz-Reina ML. Effectiveness of donepezil at six months in the treatment of cognition deterioration in patients with Alzheimer-type dementia. Rev Neurol. 2000; 31:724–728. [PubMed: 11082878]
77. Smith Doody R. Update on Alzheimer drugs (donepezil). Neurologist. 2003; 9:225–229. [PubMed: 12971832]
78. Rogers SL, Doody RS, Mohs RC, Friedhoff LT. Donepezil improves cognition and global function in Alzheimer disease: a 15-week, double-blind, placebo-controlled study. Donepezil Study Group. Arch Intern Med. 1998; 158:1021–1031. [PubMed: 9588436]
79. Galvin JE, Cornblatt B, Newhouse P, Ancoli-Israel S, Wesnes K, Williamson D, Zhu Y, Sorra K, Amatniek J. Effects of galantamine on measures of attention: results from 2 clinical trials in Alzheimer disease patients with comparisons to donepezil. Alzheimer Dis Assoc Disord. 2008; 22:30–38. [PubMed: 18317244]
80. Grossberg G, Irwin P, Satlin A, Mesenbrink P, Spiegel R. Rivastigmine in Alzheimer disease: efficacy over two years. Am J Geriatr Psychiatry. 2004; 12:420–431. [PubMed: 15249280]
81. Thomas A, Iacono D, Bonanni L, D'Andreamatteo G, Onofrj M. Donepezil, rivastigmine, and vitamin E in Alzheimer disease: a combined P300 event-related potentials/neuropsychologic evaluation over 6 months. Clin Neuropharmacol. 2001; 24:31–42. [PubMed: 11290880]
82. Bourgeois JA, Bahadur N, Minjares S. Donepezil for cognitive deficits following traumatic brain injury: a case report. J Neuropsychiatry Clin Neurosci. 2002; 14:463–464. [PubMed: 12426418]
83. Trovato M, Slomine B, Pidcock F, Christensen J. The efficacy of donepezil hydrochloride on memory functioning in three adolescents with severe traumatic brain injury. Brain Inj. 2006; 20:339–343. [PubMed: 16537276]
84. Stein TD, Montenigro PH, Alvarez VE, Xia W, Crary JF, Tripodis Y, Daneshvar DH, Mez J, Solomon T, Meng G, et al. Beta-amyloid deposition in chronic traumatic encephalopathy. Acta Neuropathol. 2015; 130:21–34. [PubMed: 25943889]
85. Mesulam MM. Neuroplasticity failure in Alzheimer's disease: bridging the gap between plaques and tangles. Neuron. 1999; 24:521–529. [PubMed: 10595506]
86. King A, Maekawa S, Bodi I, Troakes C, Al-Sarraj S. Ubiquitinated, p62 immunopositive cerebellar cortical neuronal inclusions are evident across the spectrum of TDP-43 proteinopathies but are only rarely additionally immunopositive for phosphorylation-dependent TDP-43. Neuropathology. 2011; 31:239–249. [PubMed: 21118398]
87. King A, Sweeney F, Bodi I, Troakes C, Maekawa S, Al-Sarraj S. Abnormal TDP-43 expression is identified in the neocortex in cases of dementia pugilistica, but is mainly confined to the limbic system when identified in high and moderate stages of Alzheimer's disease. Neuropathology. 2010; 30:408–419. [PubMed: 20102526]

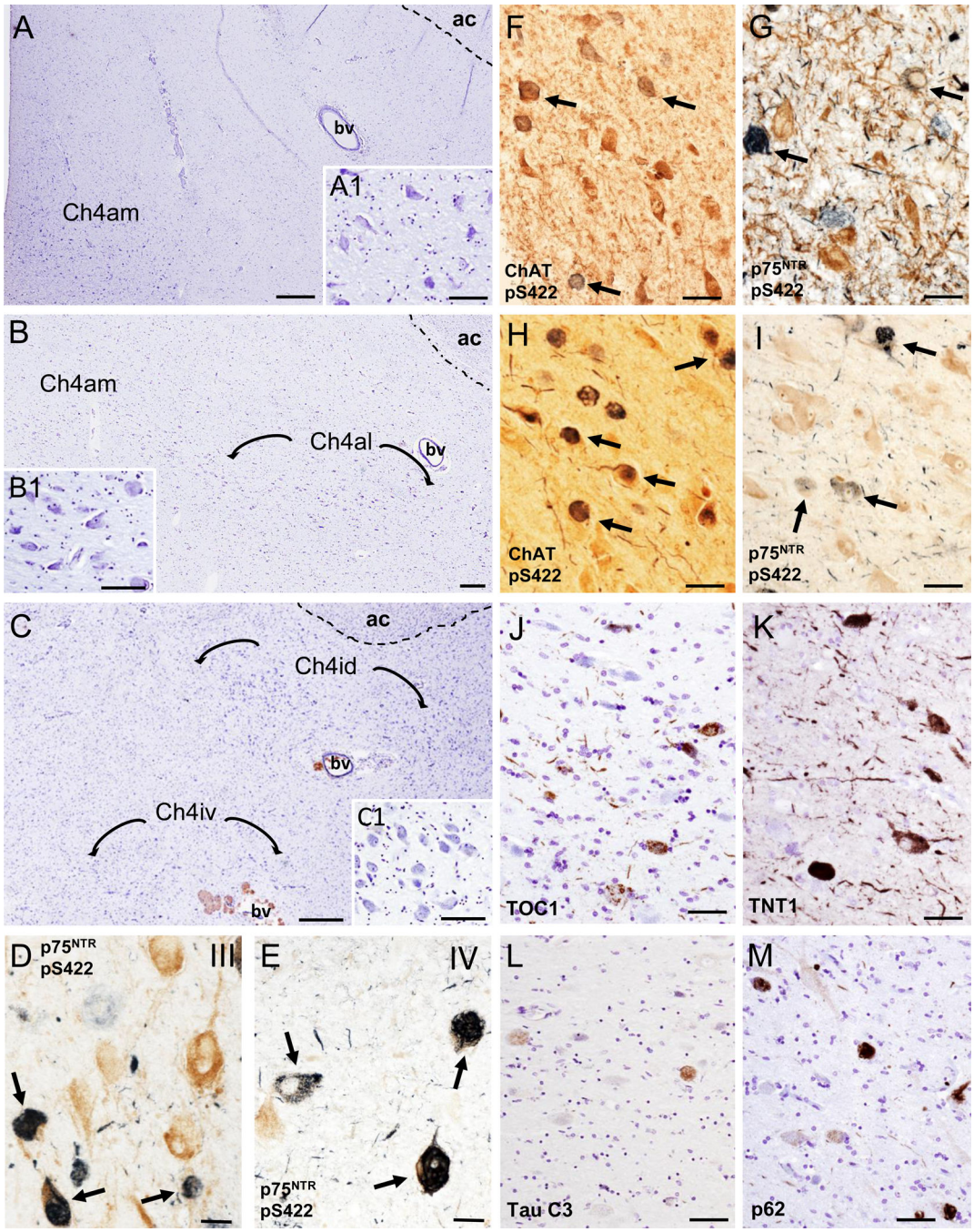

Figure 1.

Photomicrographs of cresyl violet stained sections delineating the cholinergic subfields (Ch4) examined within the nucleus basalis of Meynert (nbM) from rostral to caudal: anteromedial (Ch4am) (**A**), anterolateral (Ch4al) (**B**) and dorsal (Ch4id) and ventral (Ch4iv) intermediate (**C**); **A1, B1** and **C1**insets showing higher magnification images of Ch4am, Ch4al and Ch4id neurons from panels **A, B** and **C**respectively. **D** and **E**. Dual immunolabeled $p75^{NTR}$/pS422 neurons (dark blue; arrows) and single labeled $p75^{NTR}$ (brown) neurons in the vertical limb of the diagonal band of Broca (VDB; Ch2) in a CTE

stage III (**D**) and IV (**E**) case, respectively. **F** and **G**. Photomicrographs of ChAT (**F**) (brown) and $p75^{NTR}$-positive (brown) (**G**) neurons containing pS422-ir inclusions (dark/light blue; arrows) within the nbM anteromedial subfield in CTE stage IV. **H** and **I**. Images of the anteromedial subfield of the nbM showing dual immunolabeled ChAT (brown)/pS422 positive neurons (dark blue; arrows) and single immunolabeled ChAT neurons (brown) (**H**) and double immunolabeled $p75^{NTR}$ /pS422 positive neurons (dark and light blue; arrows) and single-labeled $p75^{NTR}$ neurons (brown) (**I**) from an AD case, respectively. **J**-**M**. Photomicrographs of TOC1 (**J**), TNT1 (**K**), Tau C3 (**L**) and p62 (**M**) positive neurons and neuropil threads in the anterior subfields of the nbM of an AD case. Note the extent of oligomer TOC1 and TNT1 positive threads compared to absence of neuropil thread Tau C3 and p62 immunostaining. Tissues were counterstained with cresyl violet in panels **J** to **M**. Abbreviations: ac, anterior commissure; bv, blood vessel. Scale bars: 500 μm (**A**), 250 μm (**B**), 200 μm (**C**), 100 μm (**B1, C1**), 80 μm (**A1**), 75 μm (**J, L, M**), 60 μm (F), 50 μm (**H, I, K**), 40 μm (**G**) and 30 μm (**D, E**).

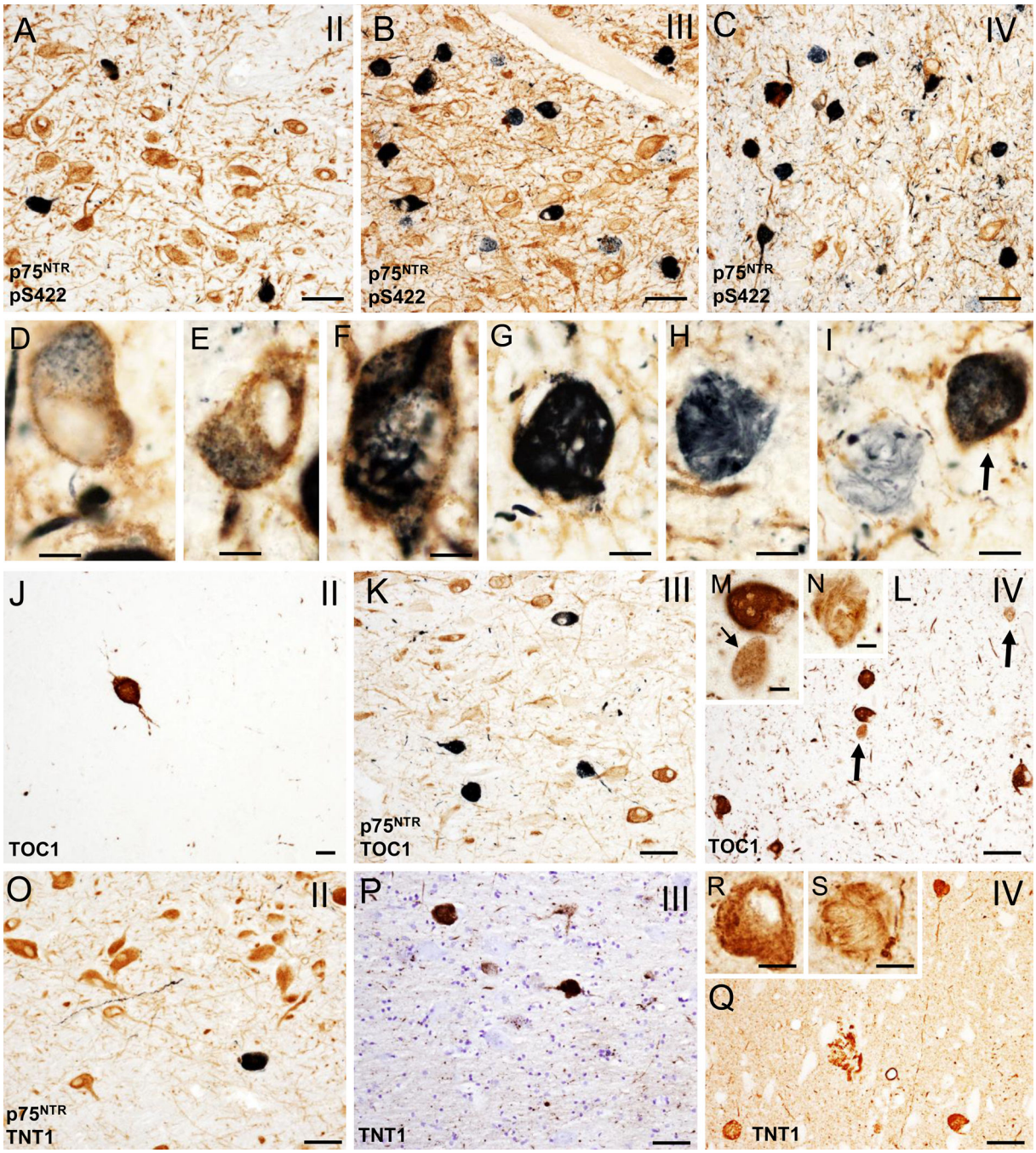

Figure 2.

A–C. Photomicrographs of tissue dual immunostained for p75^{NTR} (brown) and pS422 (dark blue/black) in the anterior subfields of the nbM showing the presence p75^{NTR} containing pS422 inclusions (dark blue) and neuropil threads (dark blue) in CTE stages II (**A**), III (**B**) and IV (**C**). Note that many more double p75^{NTR}/pS422 positive neurons and neuropil threads (dark blue) were seen in stage III and IV compared to stage II. **D–G**. High power images of double immunolabeled p75^{NTR}/pS422 neurons in the anteromedial nbM showing intraneuronal cytoplasmic pS422 imunoreactivity (black) containing granular (**D** and **E**),

filamentous (**F**) and skein of yarn-like (**G**) phenotypes in a stage IV CTE case. **H** and **I**. Twisted filamentous $p75^{NTR}$ positive inclusion (blue) resembling a skein of yarn in the nbM neuropil. Arrows indicates a double immunolabeled $p75^{NTR}$/pS422 neuron in **I**. **J–L**. Photomicrographs of single TOC1 (brown) (**J** and **L**) and dual immunolabeled $p75^{NTR}$/TOC1 (dark blue/black) neurons and neuropil threads in anterior subfields of the nbM in a stage II (**J**), III (**K**) and IV (**L**) CTE cases. Note the increase in the extent of TOC positive neuropil threads in stage IV. **M** and **N**. Insets showing higher magnification images of granular (small arrow), compact spherical (**M**) and twisted-filamentous (**N**) TOC1 immunoreactive profiles (brown) in the anterormedial subfield of the nbM neurons from panel **L** (arrows). **O–Q**. Photomicrographs of double immunolabeled TNT1/$p75^{NTR}$ (dark blue) (**O**) and single reactive TNT1 (brown) (**P** and **Q**) positive neurons and neuropil threads in the anterior subfields of the nbM from a stage II (**O**), III (**P**) and IV (**Q**) CTE cases. **R** and **S**. Insets showing details of the granular and filamentous TOC1 immunoreactivity in anteromedial subfield of the nbM neurons from a stage IV CTE case. Tissue was counterstained with cresyl violet in panel **P**. Scale bars: 75 μm (**A–C**), 65 μm (**L, O, Q**), 50 μm (**K, P**), 25 μm (**J**), 15 μm (**M, R, S**), 12 μm (**G**), 10 μm (**D, E, H**) and 8 μm (**F, I, N**).

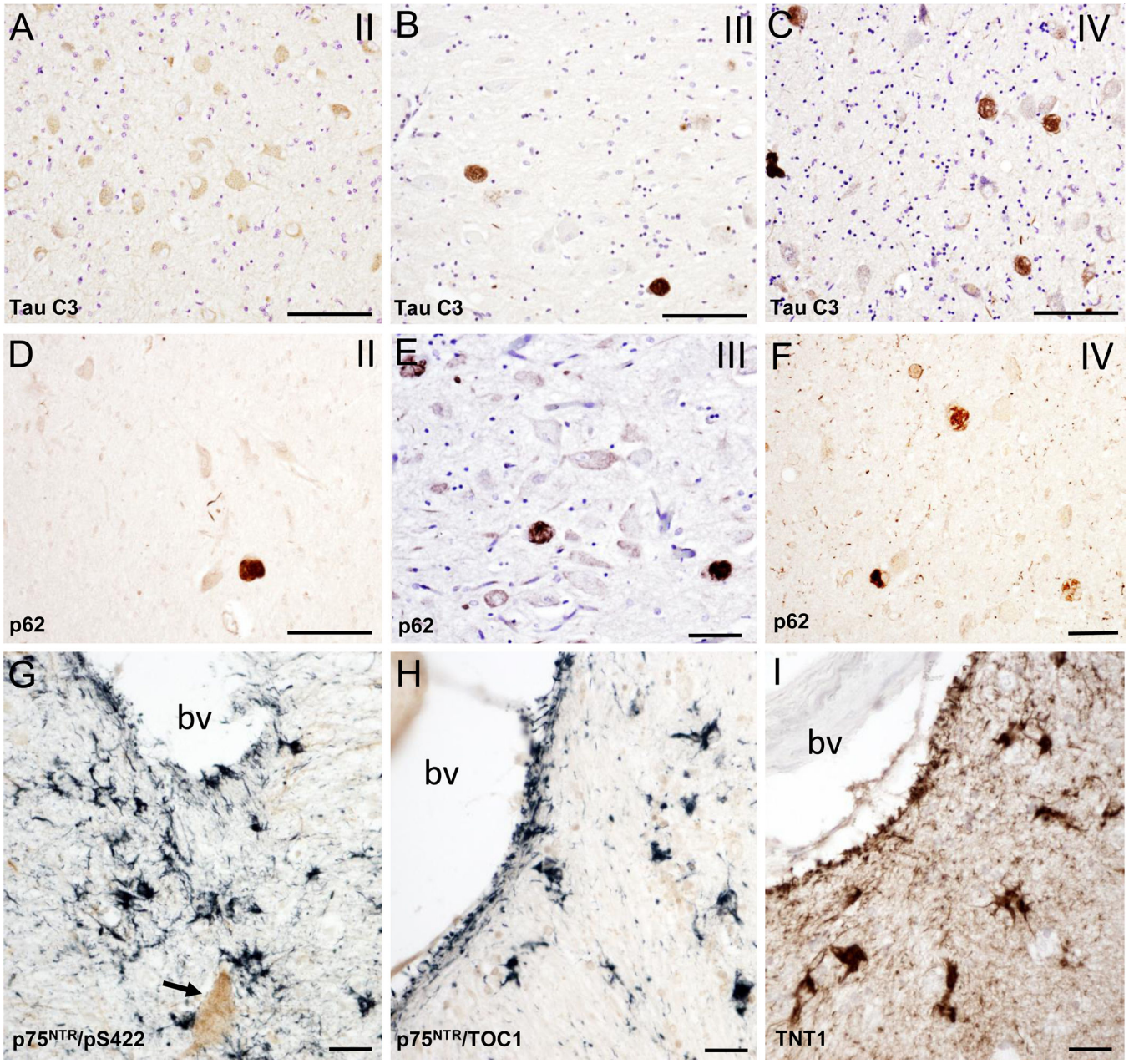

Figure 3.

Photomicrographs of Tau C3 (**A–C**) and p62 (**D–E**) immunolabeling showing many more globose Tau C3 and p62-postive neurons in the anterior subfields of the nbM in a CTE stage IV than stage II. Note the lack of nbM Tau C3 positive neurons in stage II. Photomicrographs of the double immunolabeling for pS422/$p75^{NTR}$ (**G**), TOC1/$p75^{NTR}$ (**H**) and single immunolabeling for TNT1 (**I**) showing pS422 (blue), TOC1 (blue) and TNT1 (brown) immunostained astrocytes near to a blood vessel in anteromedial subfield of the nbM in a CTE stage IV case. Arrow indicates a $p75^{NTR}$ positive cholinergic neuron. Abbreviation: bv, blood vessel. Tissues in panels **A, B** and **E** were counterstained with cresyl violet. Scale bars: 90 μm (**A–D**), 70 μm (**E, F**), 40 μm (**G**) and 25 μm (**H, I**).

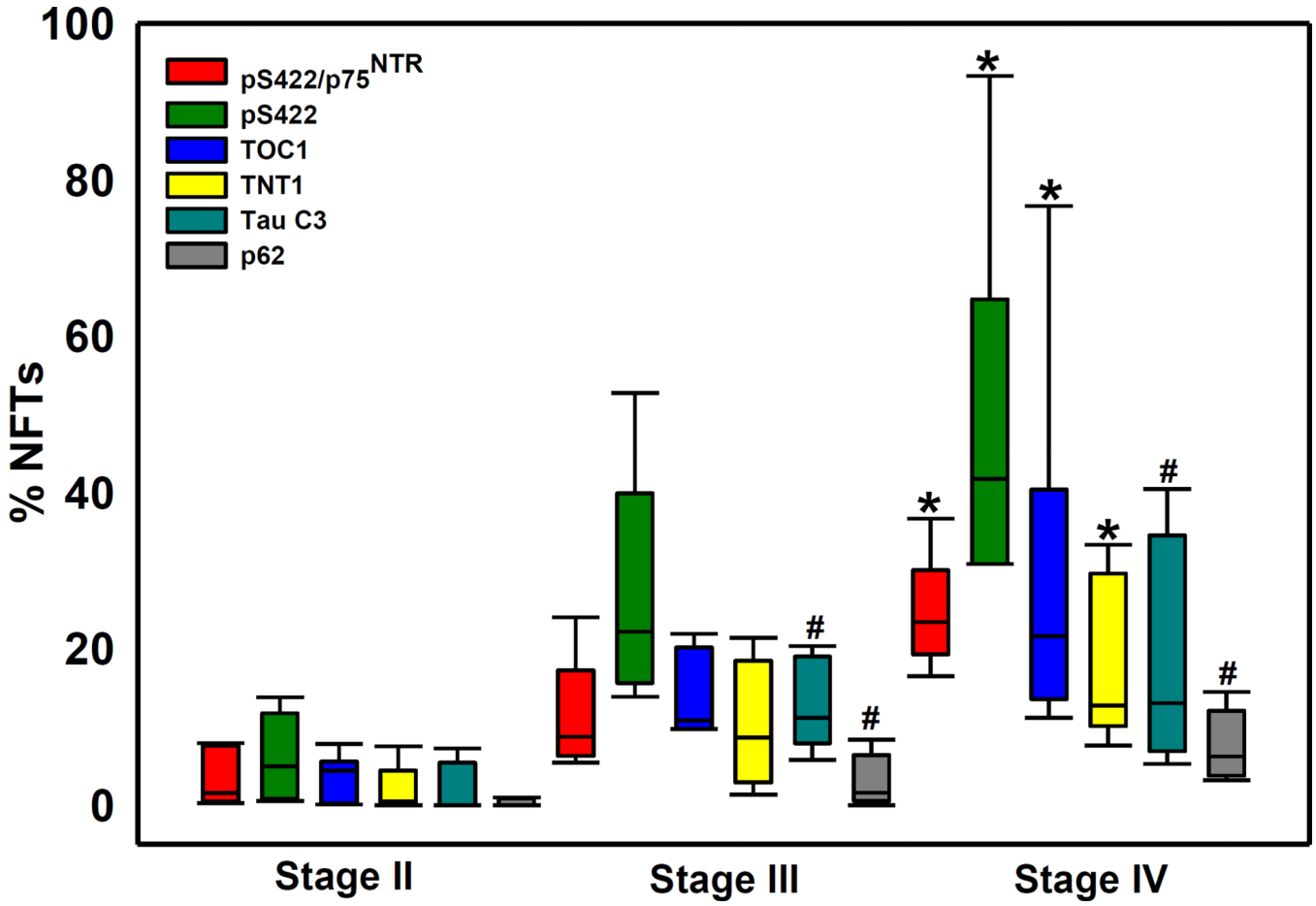

Figure 4.

Box plot showing the percent of double pS422/p75^{NTR} as well as single pS422, TOC1, TNT1, Tau C3 and p62 immunopositive neurofibrillary tangle (NFTs) relative to the total number of p75 ^{NTR} positive neurons in nbM in stages II, III and IV. Percentage of pS422/p75^{NTR}, pS422, TOC1, TNT1positive NFTs were significantly increased in stage IV compared to stage II (*, $p<0.01$), while the percentage of Tau C3 and p62 NFTs were significantly higher in stage IV and III compared to stage II (#, $p<0.01$).

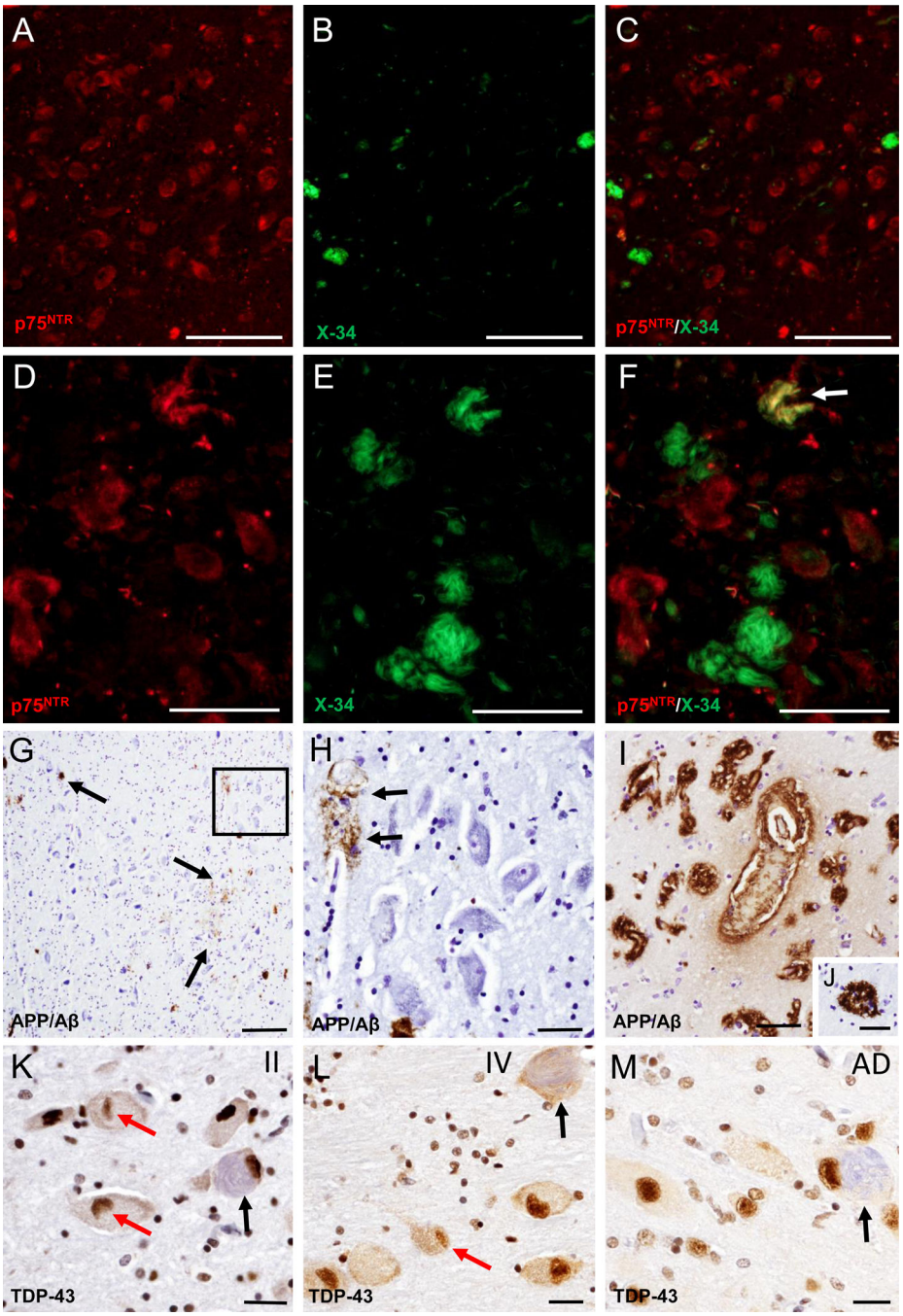

Figure 5.

A–F. Fluorescence images of single $p75^{NTR}$ (red) (**A** and **D**) and X-34 (green) (**B** and **E**) staining and merged-images (**C** and **F**) showing limited of X-34 positive neurons (**B**) and the absence of double $p75^{NTR}$/X-34 positive neurons (**C**) in the nbM in a CTE stage II case, while many more fibrillary X-34 positive neurons (**E** and **F**) were seen in the anterior subfields of the nbM in a CTE stage IV case. Arrow in **F** indicates a double immunolabeled $p75^{NTR}$/X-34 neuron (yellow). **G**. Low magnification image of scattered APP/Aβ (6E10) labeled deposits (brown; arrows) in the nbM anteromedial subfield of a CTE stage IV case.

H. High power image of APP/Aβ-positive blood vessel (arrows) from the area boxed in panel **G**; note the lack of intraneuronal APP/Aβ immunostaning in the large hyperchromic nbM neurons (blue). **I–M**. Images showing APP/Aβ positive deposits in blood vessels (bv) in the insular cortex as well as APP/Aβ reactive cored neuritic plaques in the temporal cortex (**J**) from a stage IV CTE case. **N**. **K–M**. Images showing nuclear TDP-43 staining (brown) in the nbM neurons from a CTE stage II (**K**), IV (**L**) and an AD case (**M**). Note the presence of lenticular shaped TPD-43-ir inclusions (red arrows) within nbM neurons in a CTE stage II (**K**) and IV (**L**), but not in the AD case (**M**). Black arrows indicate NFT-containing neurons (light blue) in CTE and AD cases. Sections in panels **K–M** were counterstained with hematoxylin. Scale bars: 200 μm (**G**), 100 μm (A–C), 50 μm (**D–H, J**), 40 μm (**I**), 25 μm (**K–M**)

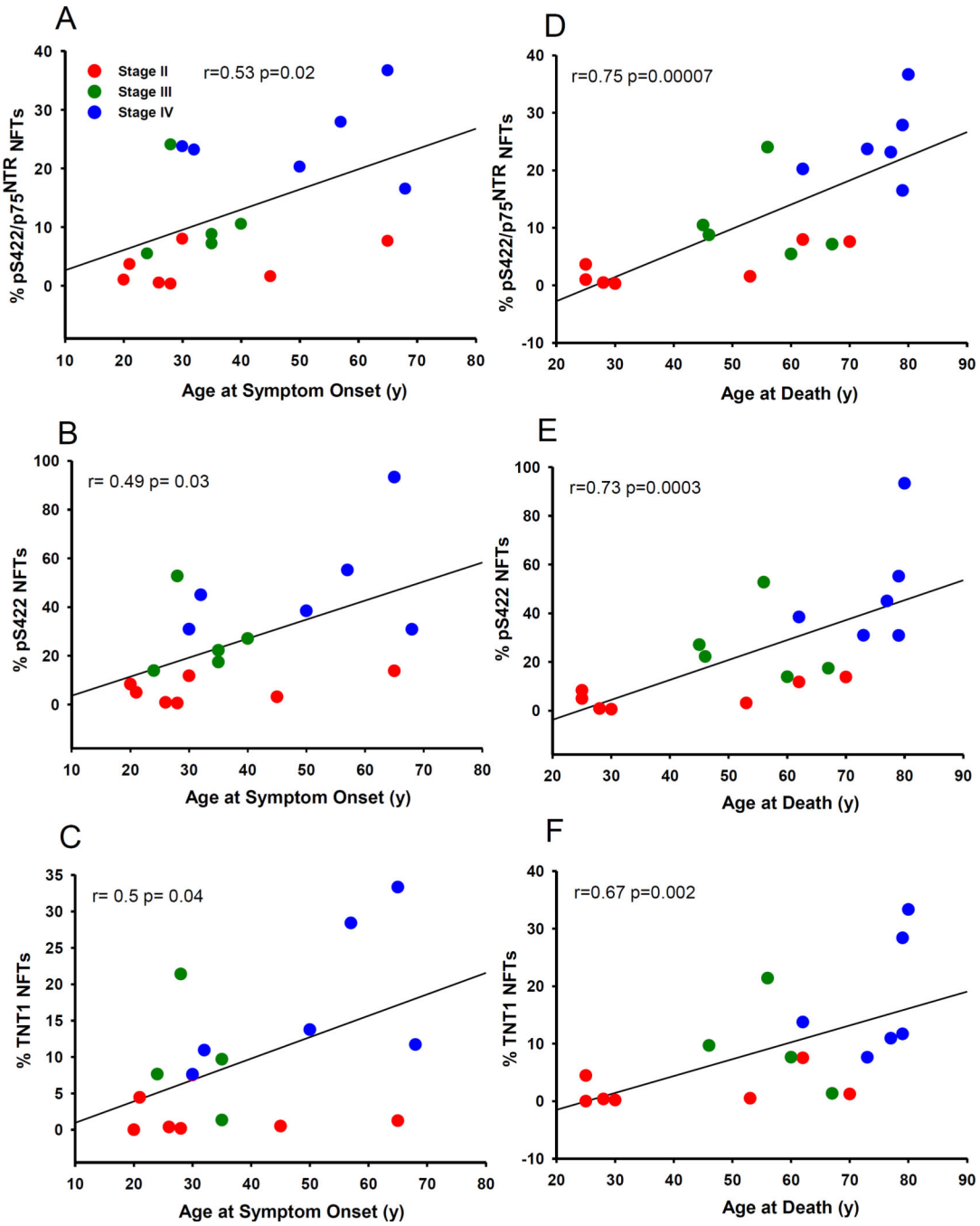

Figure 6.

Percent of pS422/p75^{NTR} (**A** and **D**), pS422 (**B** and **E**) and TNT1 (**C** and **F**) positive NFTs in the nbM correlated positively with the age of symptom onset (**A–C**) and age at death (**D–F**) across CTE stages. Stage II, red circles; Stage III, green circles; Stage IV, blue triangles.

Brain Inj. Author manuscript; available in PMC 2017 March 13.

Table 1

Demographics

Stage	Gender	Race	Sport/act	Age Sport Begun (y)	Years Play	Age at Onset Symptoms (y)	Interval between retirement and symptoms (y)	Interval between symptom onset and death (y)	Age at Death (decade)
II	**M**	**C**	**Prof. Football**	16	15	65	34	5	7
	M	**AA**	**Prof. Football**	11	10	45	24	8	5
	M	**C**	**Prof. Football**	9	20	28	−1	2	3
	M	**C**	**Semi-prof. Football**	8	18	30	4	32	6
	M	**C**	**Prof. Hockey**	4	24	26	−2	2	2
	M	**C**	**College Football**	6	15	21	0	4	2
	M	**C**	**HS Football, Wrestler, Pole-Vaulter**	6	11	20	3	5	2
III	**M**	**AA**	**Prof. Football**	10	17	28	1	28	5
	M	**C**	**Prof. Football**	11	23	35	1	11	4
	M	**C**	**Prof. Football**	14	17	35	4	32	6
	M	**C**	**Prof. Football**	10	21	40	9	5	4
	M	**C**	**Prof. Football**	14	15	24	−5	36	6
IV	**M**	**AA**	**Prof. Boxer**	12	19	30	−1	43	7
	M	**C**	**Prof. Football**	10	30	57	17	22	7
	M	**C**	**Prof. Football**	16	13	68	39	11	7
	M	**AA**	**Prof. Football**	9	22	50	19	12	6
	M	**AA**	**Prof. Football/Veteran**	14	23	65	28	15	8
	M	**C**	**Prof. Football/Veteran**	15	15	32	2	45	7

AA, African American; C, Caucasian; HS, High School; M, male; Semi-prof, Semiprofessional; Prof, Professional

Table 2

Progression of symptoms by CTE pathological stage

	II	III	IV	*p-value*[a]	Pairwise comparison
Age Sport Begun (y)	8.57 ± 3.98 *	11.80 ± 2.0	12.66 ± 2.8	ns	--
Years of Play	16.14 ± 4.9	18.60 ± 3.2	20.33 ± 6.1	ns	--
Age at Onset Symptoms (y)	33.57 ± 16.1	32.40 ± 6.3	50.33 ± 16.2	ns	--
Interval Between Retirement and Symptoms (y)	8.85 ± 14.2	2.00 ± 5.09	17.33 ± 15.2	ns	--
Interval Between Symptom Onset and Death (y)	8.28 ± 10.6	22.40 ± 13.6	24.66 ± 15.4	ns	--
Age at Death (y)	41.85 ± 19.2	54.80 ± 9.3	75.00 ± 6.8	0.002	II < IV

*mean ± SD

[a]One-way ANOVA with Holm-Sidak post *hoc*

Table 3

Correlation between symptoms and death by CTE pathological stage

	Years of Play	Age at Onset Symptoms (y)	Interval between retirement and symptoms (y)	Interval between symptom onset and death (y)	Age at Death (y)
Age at Sport Begun	--	r= 0.60 p= 0.008	ns	r= 0.48 p= 0.04	r= 0.72 p= 0.0003
Years of Play	--	--	ns	ns	ns
Age at Onset Symptoms (y)	--	--	r= 0.85 p< $1*10^{-6}$	ns	r= 0.71 p= 0.0005
Interval between retirement and symptoms (y)	--	--	--	ns	r= 0.52 p= 0.02
Interval between symptom onset and death (y)	--	--	--	--	r= 0.64 p= 0.003

ns, no significance

Table 4

Percent of double pS422/p75 and single pS422, TOC1, TNT1, Tau C3 and p62 NFTs within the nbM by CTE pathological stage

	II	III	IV	*p-value*	pairwise comparison
pS422/p75	3.19 ± 3.30 *	11.16 ± 7.4	24.68 ± 6.9	0.002 *a*	II<IV
pS422	6.18 ± 5.2	26.65 ± 15.4	48.90 ± 23.6	0.001 *a*	II<IV
TOC1	3.62 ± 2.9	14.13 ± 5.6	28.95 ± 24.3	0.001 *a*	II<IV
TNT1	2.03 ± 2.8	10.01 ± 8.3	17.62 ± 10.5	0.008 *b*	II<IV
Tau C3	1.80 ± 3.1	13.00 ± 5.9	15.64 ± 11.8	0.009 *b*	II<III, IV
p62	0.36 ± 0.4	3.10 ± 3.3	8.69 ± 4.4	0.002 *b*	II<III, IV

*mean ± SD

*a*Kruskal-Wallis with Dunn's post *hoc*

*b*One-way ANOVA with Holm-Sidak post *hoc*

Table 5

Correlation between the percentage of tau and autophage NFTs within the nbM by CTE pathological stage

	pS422	TOC1	TNT1	Tau C3	p62
pS422/p75NTR	r= 0.96 p< $1*10^{-6}$	r= 0.93 p< $1*10^{-6}$	r= 0.91 p< $1*10^{-6}$	r= 0.86 p< $1*10^{-6}$	r= 0.81 p< $1*10^{-6}$
pS422	--	r= 0.97 p< $1*10^{-6}$	r= 0.91 p< $1*10^{-6}$	r= 0.86 p< $1*10^{-6}$	r= 0.80 p< $1*10^{-6}$
TOC1	--	--	r= 0.90 p< $1*10^{-6}$	r=0.88 p< $1*10^{-6}$	r= 0.81 p< $1*10^{-6}$
TNT1	--	--	--	r= 0.75 p<$1*10^{-4}$	r= 0.81 p< $1*10^{-6}$
Tau C3	--	--	--	--	r= 0.67 p= 0.002

Table 6

Correlation between percentage of NFTs and symptom progression by CTE pathological stage

	Age at Sport Begun	Years of Play	Age at Onset Symptoms (y)	Interval between retirement and symptoms (y)	Interval between symptom onset and death (y)	Age at Death (y)
pS422/p75NTR	ns	ns	r= 0.53 p= 0.02	ns	r= 0.61 p= 0.006	r= 0.75 p= 0.00007
pS422	ns	ns	r= 0.49 p= 0.03	ns	r= 0.62 p= 0.005	r= 0.73 p= 0.0003
TOC1	ns	ns	ns	ns	r= 0.62 p= 0.05	r= 0.65 p= 0.003
TNT1	ns	ns	r= 0.5 p= 0.04	ns	r= 0.54 p= 0.02	r= 0.67 p= 0.002
Tau C3	ns	ns	ns	ns	r= 0.67 p= 0.002	r= 0.65 p= 0.004
p62	ns	ns	ns	ns	r= 0.68 p= 0.002	r= 0.51 p= 0.03

ns, no significance